CHAPTER 5

An improved model to study tumor cell autonomous metastasis programs using MTLn3 cells and the Rag2$^{-/-}$ $\gamma c^{-/-}$ mouse

Sylvia Le Dévédec, Wies van Roosmalen, Naomi Maria, Max Grimbergen, Chantal Pont, Reshma Lalai and Bob van de Water

Division of Toxicology, Leiden Amsterdam Center for Drug Research, Leiden University, Leiden, the Netherlands.

Published in *Clin. Exp. Metastasis*, May 2009

ABSTRACT

Treatment of breast cancer metastases remains a problem since the underlying mechanisms leading to these secondary tumor deposits are still poorly understood. To study the processes of metastasis, a good in vivo tumor metastasis model is required. Here, we show that increased expression of the EGF receptor in the MTLn3 rat mammary tumor cell-line is essential for efficient lung metastasis formation in the Rag mouse model. EGFR expression resulted in delayed orthotopic tumor growth but at the same time strongly enhanced intravasation and lung metastasis. Previously, we demonstrated the critical role of NK cells when using the MTLn3 cell-line to study experimental lung metastasis formation in syngenic F344 rats. But this model is incompatible with human EGFR. Using the highly metastatic overexpressing EGFR MTLn3 cell-line, we report that only the Rag2$^{-/-}\gamma c^{-/-}$ mice, which lack NK cells, allow efficient lung metastasis from primary tumors in the mammary gland while remaining innate immune cells in nude and SCID mice reduce MTLn3 lung metastasis formation. In addition, we confirm this finding with the orthotopic transplantation of the 4T1 mouse mammary tumor cell-line. Thus, we have established an improved in vivo model using a Rag2$^{-/-}$ $\gamma c^{-/-}$ mouse strain together with MTLn3 cells that have increased levels of the EGF receptor, which enables us to study tumor cell autonomous mechanisms underlying lung metastasis formation. This improved model can be used for drug target validation and development of new therapeutic strategies against breast cancer metastasis formation.

1. Introduction

Breast cancer is the most common cause of cancer among women and the second leading cause of cancer deaths in Western countries. The metastatic spread of tumor cells from their primary site to distant organs in the body is the principal cause of mortality[1]. Thus, understanding metastasis is one of the most significant problems in cancer research[2-4]. It is an important challenge to develop suitable animal models to enhance our understanding of the mechanisms that underlie metastatic progression and to evaluate treatments for metastatic diseases[5].

Currently available *in vivo* models of breast tumor progression and metastasis include transplantable models and genetically engineered mice that develop primary and metastatic cancers[5-8]. Transplantable tumor models include syngeneic models, in which the cancer cell line/tissue transplanted is of the same genetic background as the animal, and xenograft models referring to human cancer cell lines/ tissues transplanted into immunocompromised hosts, such as nude and severe combined immunodeficient mice[5]. Breast xenograft tumors are produced by injecting breast cancer cells into the flank (subcutaneous) or preferably into the mammary fat pad (orthotopic) of a female animal. Subcutaneous xenograft mouse models are typically the standard for cancer drug screening in the pharmaceutical industry[9], but the use of orthotopic xenotransplantation models should be favored since tissue specific stromal cell interactions play a crucial role in the biology of cancer progression and metastasis.

Metastasis is a consequence of multiple steps, including growth of a primary tumor, intravasation, arrest and growth in a secondary site[2,3]. The study of metastasis not only requires a relevant mouse model, it requires first a suitable cell line. The rat mammary adenocarcinoma cell line MTLn3 is an excellent model to study breast cancer progression and treatment[10,11]. It is also known that the epidermal growth factor receptor (EGFR, also refered as ErbB1) is often overexpressed in breast cancer and results not only in uncontrolled cell proliferation[12,13] but also in increased tumor cell motility and invasion[14-16]. Since we want to study intravasation leading to metastasis formation, we evaluate the effect of enhanced ErbB1 signalling in the MTLn3 cells when using the orthotopic Rag mouse breast cancer model.

Efficient metastasis formation is, on the one hand, dependent on tumor cell autonomous biological programs that define migration, intravasation survival and extravasation[14]. On the other hand, for xenotransplantation models, immune cell responses to foreign antigens on the injected tumor cells should be eliminated. Therefore, to understand the complexity of the tumor cell autonomous biological programs involved in metastasis formation, it is important to use immunocompromised hosts that exclude interference by the immune system.

The most widely used immunodeficient mice (nude and SCID) lack the adaptive immune response. However, these mice still harbour large numbers of cells of the innate immune system, including Natural Killer cells[17]. These cells are

important in the killing of viable circulating tumor cells, thus preventing metastasis formation of tumor cells that otherwise efficiently escape the primary tumor through enhanced invasion and intravasation programs[18,19-25]. Indeed, we showed previously that the MTLn3 cells are killed by the circulating NK-cells in Fischer 344 rats, thus preventing efficient lung metastasis formation. Although pretreatment with NK depleting antibodies allowed experimental lung metastasis formation in this model[26,27], continuous NK depleting antibody injection does not fit the requirements for easy and efficient orthotopic breast/tumor metastasis models. To study breast tumor progression and metastasis formation using the MTLn3 expressing EGF receptor cells, an appropriate animal model with a compromised innate and adaptive immune system is still needed.

The goal of the current study was to develop an MTLn3 cell breast tumor metastasis animal model that allows the unbiased analysis of tumor cell-dependent metastasis programs, independent of adaptive and innate immune system surveillance. We first show that increased expression of ErbB1 receptor in MTLn3 was required for lung metastasis formation in Rag2$^{-/-}\gamma c^{-/-}$ mice. Secondly, by comparing different immune deficient mouse models, we confirm that Rag2$^{-/-}$ $\gamma c^{-/-}$ mice, which lack NK cells, are an excellent recipient animal model for the MTLn3 and 4T1 cells to study the metastasis process. In conclusion, we have established an improved animal model that can be used to study the biological steps that are essential in the formation of distant metastasis.

2. Materials and Methods

2.1 Cell lines

MTLn3 rat mammary adenocarcinoma cells[28] were cultured as previously described[29]. MTLn3-GFP-ErbB1 and MTLn3-GFP cell-lines were previously described[16] and were maintained in αMEM (Life Technologies, Inc., Gaithersburg, MD) supplemented with 5% fetal bovine serum (Life Technologies). The mouse mammary metastatic 4T1-luc cell-line was purchased from Caliper Lifescience and cultured in RPMI-1640 supplemented with 10% fetal bovine serum (Life Technologies).

2.2 Reagents

Mouse anti-human ErbB1 was purchased from Calbiochem (EMD Biosciences, San Diego,CA). Rabbit anti-human ErbB1 used for immunoblotting was purchased from Cell Signaling Technology. Goat anti-mouse APC was purchased from Cedarlane (Ontario, CA). Alpha modified minimal essential medium (a-MEM), Fetal Bovine Serum (FBS), phosphate buffered saline (PBS) and trypsin were from Life Technologies (Rockville, MD, USA).

2.3 ErbB1 staining

Flow cytometry: MTLn3 were harvested and incubated for 45 minutes with 50 µl of mAb ErbB1 (2µg/ml in PBS). The cells were washed with cold PBS and incubated for 45 minutes with the secondary antibody goat-anti mouse APC in PBS (2µg/ml). Finally, the cells were washed and suspended in 0.3 mL PBS. ErbB1 and GFP expression were analysed on the FACScalibur (Becton Dickinson).
Immunoblotting: Cells were scraped in ice-cold TSE (10 nM Tris-HCl, 250 mM sucrose, 1 mM EGTA, pH 7.4) supplemented with inhibitors. After sonication of either cells or tissue, protein concentrations were determined by the Bio-Rad (Hercules, CA) protein assay using IgG as a standard. Equal amounts of total cellular protein were separated by 7.5% SDS-PAGE and transferred to polyvinylidene difluoride membranes (Millipore, Billerica, MA). Blots were blocked with 5% (w/v) bovine serum albumin in TBST [0.5 mol/L NaCl, 20 mmol/L Tris-HCl, 0.05% (v/v) Tween 20 (pH 7.4)] and probed with primary antibody (overnight, 4°C) followed by incubation with secondary horseradish peroxidase–coupled antibody and visualized with Enhanced Chemiluminescence Plus reagent (Amersham Biosciences, Uppsala, Sweden) by scanning on a multilabel Typhoon imager 9400 (Amersham Biosciences).

2.4 Animals

Female BALB/c nu/nu, SCID [CB17/lcr-Prkdc^{scid}/Crl] and SCID Beige [CB17/lcr.Cg-Prkdc^{scid} Lyst^{bg}/Crl] mice aged between 6 and 7 weeks were purchased from Charles River (L'Arbresle, France). BALB/c mice aged between 6 and 7 weeks were purchased from Janvier (Uden, The Netherlands). 6-week old Rag2$^{-/-}$ γc$^{-/-}$ mice were obtained from in house breeding. Animals were housed in individually ventilated cages under sterile conditions containing 3 mice per cage. Sterilised food and water were provided ad libitum.

2.5 Spontaneous and experimental metastasis assays.

To measure spontaneous metastasis, tumor cells were grown to 70% to 85% confluence before being harvested for cell counting. Cells (5 x 10^5 for the MTLn3 or 1 x 10^5 for the 4T1-luc) were injected into the right thoracic mammary fat pads of the different mouse strain. The cells were injected in a volume of 100 µL of PBS without Ca^{2+} and Mg^{2+} through a 25-gauge needle. Tumor growth rate was monitored at weekly intervals after inoculation of tumor cells. Horizontal (h) and vertical (v) diameters were determined, and tumor volume (V) was calculated ($V=4/3\pi(1/2[\sqrt{(h*v)}]^3$). After 3 or 4 weeks, the animals were anesthetized with pentobarbital and the lungs were excised and rinsed in ice-cold PBS. For the GFP labeled MTLn3 cell-lines, the right lung was used to count the tumor burden. For rough estimation, the right lungs were imaged with the Fluorescent Imaging unit

IVIS (see below). And for detailed quantification, the flat side of the right lung was analysed with the immunofluorescence microscope. With a x10 objective lens, we screened the flat surface of the lobe and counted the number of GFP positive metastases. Following that step, the right lung was cut into two pieces and fixated in liquid nitrogen (used to prepare tissue homogenates for immunoblot analysis) and 4% paraformaldehyde. The left lung was injected with ink solution and thereafter destained in water and fixated in Fekete's (4.3% (v/v) acetic acid, 0.35% (v/v) formaldehyde in 70% ethanol). For the 4T1-luc cell-line, the lung tumor burden was quantified by counting the number of surface metastases, white spots on the ink injected left lung. For the experimental lung metastasis assay, 2 x 10^5 MTLn3 cells were injected into the lateral tail veins of 5- to 7-week-old female Rag2$^{-/-}\gamma c^{-/-}$ mice. Three to four weeks after injection, the mice were euthanized, and the lungs were removed and subjected to fluorescent imaging and histologic examination as described below.

2.6 Fluorescent imaging

Fluorescent imaging (FLI) was performed with a highly sensitive, cooled CCD camera mounted in a light-tight specimen box (IVIS™; Xenogen). Imaging and quantification of signals were controlled by the acquisition and analysis software Living Image® (Xenogen). For *ex vivo* imaging, lungs were excised, placed into a petri dish, and imaged for 1–2 min. Tissues were subsequently fixed as mentioned above and prepared for standard histopathology evaluation.

2.7 Measurement of tumor cell blood burden

At the end point of the MTLn3 spontaneous metastasis assay, mice were sacrificed with Nembutal. The right chest was exposed by a simple skin flap surgery. Blood was taken from the right atrium via heart puncture with a 25-gauge needle and 1-mL syringe coated with heparin. Blood (0.2 - 1.0 mL) was harvested from each animal. The blood was immediately plated into 100-mm-diameter dishes filled with 5% fetal bovine serum/αMEM growth medium. The next day, the plates were rinsed with fresh medium containing 0.8 mg/mL geneticin to selectively grow the tumor cells. After 3 to 7 days, all dishes were scanned for GFP expression with the Typhoon imager 9400 (Amersham Biosciences). The tumor cell clones were counted by image analysis of the scan made of the dishes. Tumor blood burden was calculated as total colonies in the dish divided by the volume of blood taken.

2.8 Tumor histology and quantitative assessment of the efficiency of metastasis

The primary tumors and lungs from each mouse were used for histologic analysis. Samples were fixed in formalin and embedded in paraffin, and 5-µm sections were stained with H&E.

2.9 Statistical analysis

Student's *t* test was used to determine if there was a significant difference between two means ($P < 0.05$). Values are presented as mean ± SD. Significant differences are marked in the graphs.

3. Results

3.1 ErbB1 overexpression in MTLn3 cells delays tumor growth but facilitates breast cancer lung metastasis formation in Rag2 $^{-/-}$ $\gamma c^{-/-}$ mice

Since the EGF receptor is often over expressed in breast cancer progression[12,13], we wanted to use MTLn3-GFP-ErbB1 cells, because of the high likelihood of success for metastasis formation. First, we verified whether ErbB1 overexpression is indeed essential for metastases formation in the Rag mouse model. Therefore we compared MTLn3-GFP with MTLn3-GFP-ErbB1 cells. Increased expression of ErbB1 protein in the MTLn3-GFP-ErbB1 cell-line was confirmed by Western blot (Fig. 1A) and flow cytometry (Fig 1B). We also checked that GFP was equally expressed in both cell-lines (Fig. 1B). The expression of GFP was used to count the lung metastases and detect the tumor cells in blood. To determine the effects of increased ErbB1 expression on tumor growth and metastasis, MTLn3-GFP-ErbB1 and control cell-line MTLn3-GFP were injected into the mammary fat pads of Rag2$^{-/-}$ $\gamma c^{-/-}$ mice, and tumor growth was monitored. All animals implanted with tumor cells formed tumors at the site of injection. The tumor growth of the MTLn3-GFP cells was faster than of the MTln3-GFP-ErbB1 cells (Fig. 1C). Animals were sacrificed when the primary tumor reached similar volume for the two cell–lines between day 25 and 30. Indeed, there was no significant difference in tumor weight at the time of sacrifice (Fig. 1D). The animals were checked for spontaneous metastasis efficiency. Mice implanted with MTLn3-GFP-ErbB1 cells had significantly more lung metastases than mice implanted with MTLn3-GFP cells (Fig.2A) also evidence by fluorescence imaging (Fig.2B). Histological analysis of the lungs did show the absence of micro metastases in the MTLn3-GFP group (Fig.2C). In the lungs of mice implanted with MTLn3-GFP-ErbB1 cells, many macro metastases could be detected on the surface and also through the lungs (Fig. 2C). No correlation was founded between tumor weight and number of lung metastases (Fig. 2D). The extra days given to the mice with a delay in tumor

growth could possibly explain the increased number of lung metastases in the MTLn3-GFP-ErbB1 group. Therefore, we performed an experiment where we sacrificed both groups exactly at the same time (25 days). The primary tumors of the MTLn3-GFP-ErbB1 group showed again reduced growth rate (supplementary data figure 2A) and tumor weight was much lower than the MTLn3-GFP tumors (Fig. S2B). Despite this reduced tumor growth, there was a trend that the number of lung metastases was higher in ErbB1-expressing tumor bearing mice (Fig.S2C). In conclusion, increased expression of ErbB1 in the MTLn3 cells results in reduced tumor growth but increased number of lung metastasis in the Rag mouse.

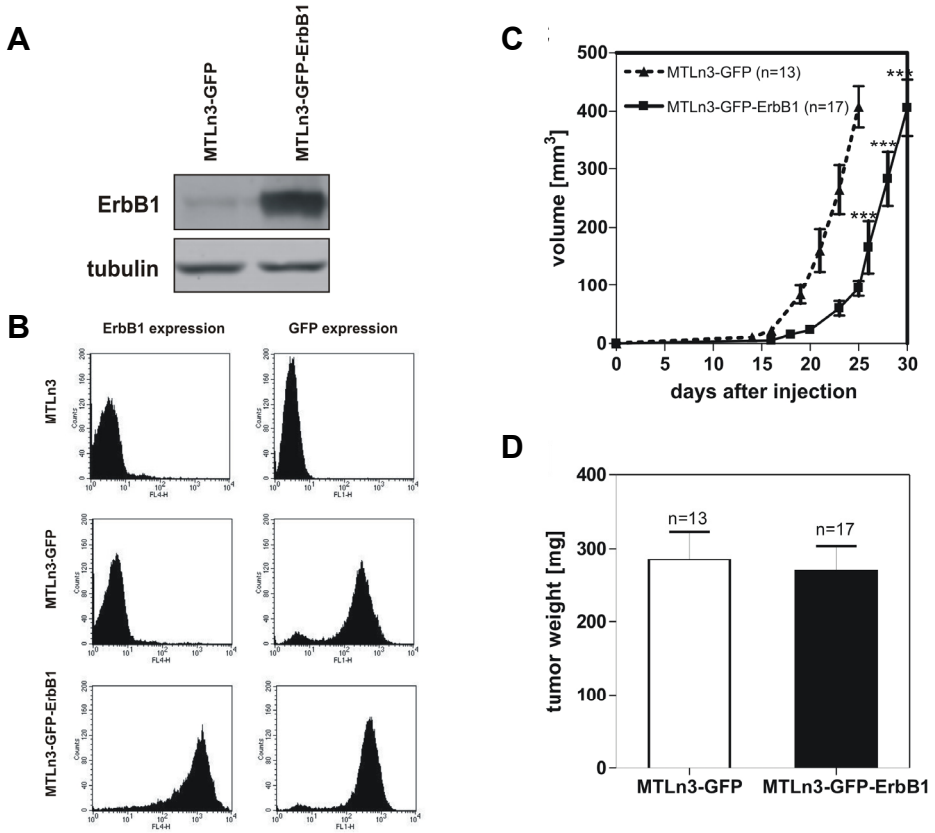

Figure 1: ErbB1 over-expression does affect tumor growth rate of MTLn3 in a spontaneous metastasis assay. (A) Western blot of ErbB1 expression in MTln3-GFP and MTLn3-GFP-ErbB1 cell-lines. (B) Fluorescence-activated cell sorting (FACS) analysis of cell surface expression levels of human ErbB1 and GFP expression levels for MTLn3-GFP and MTLn3-GFP-ErbB1 cell-lines. (C) Primary tumor growth measured by caliper during spontaneous metastasis assay. Rag mice were inoculated with MTLn3-GFP (n=13) and MTLn3-GFP-ErbB1 (n=17) cells (MTln3-GFP-ErbB1 versus MTLn3-GFP, P< 0.0001). (D) Primary tumor weight at the end point of the spontaneous metastasis assay (P>0.05).

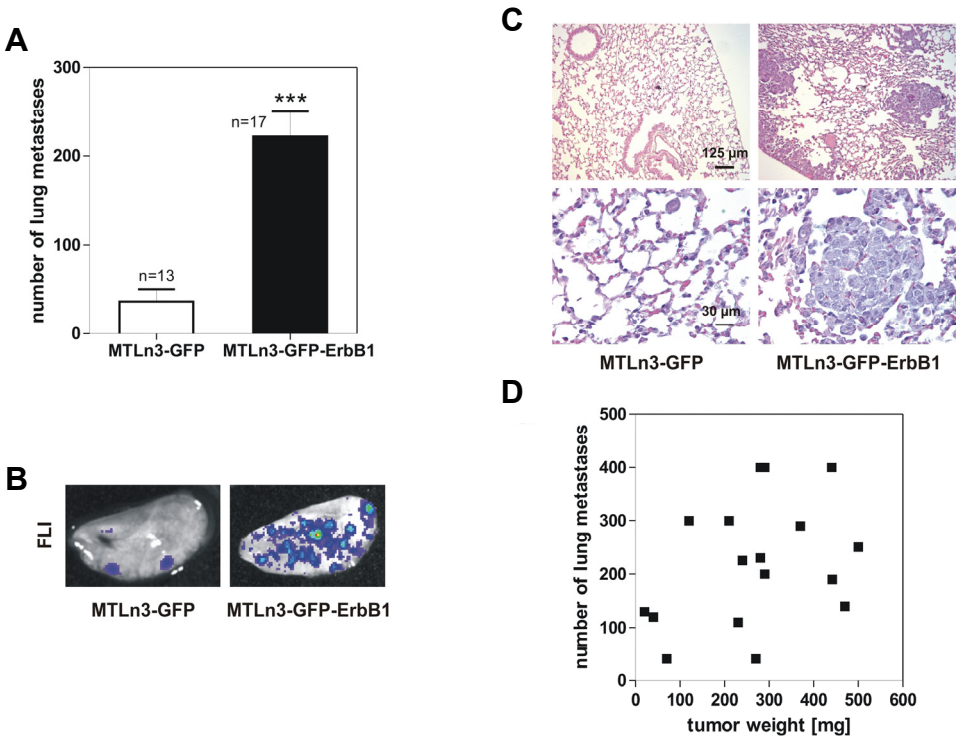

Figure 2: ErbB1 over-expression significantly enhances lung metastasis formation which is not dependent on tumor weight. (A) Lung metastases counted with a fluorescent microscope at x10 magnification (only one side of the left lung) at the end point of the spontaneous metastasis assay (MTln3-GFP-ErbB1 versus MTLn3-GFP, P< 0.0001). (B) Lung metastases visualized with the FLI (GFP detection) after spontaneous metastasis assay with the MTLn3-GFP and the MTLn3-GFP-ErbB1 cells. (C) H&E staining of lung tissue of MTLn3-GFP (left panel) and MTLn3-GFP-ErbB1 cells (right panel) injected mice. (D) Lung metastases plotted against tumor weight of MTLn3-GFP-ErbB1 tumors bearing mice (n=17).

3.2 ErbB1-driven metastasis in the Rag2$^{-/-}$ γc$^{-/-}$ mice is dependent on enhanced intravasation in the primary tumor.

Intravasation is a crucial step in the process of metastasis formation where ErbB1 signalling is thought to be a key player. Intravasation can be evaluated by determining the number of tumor cells present in blood collected from the right atrium of the heart, before filtration by the lungs. Animals bearing MTLn3-GFP tumors had very few tumor cells/mL of blood, whereas animals bearing MTLn3-GFP-ErbB1 tumors had an average of 170 tumor cells/ml of blood (Fig. 3A and B). In conclusion, increased ErbB1 expression in MTLn3 cells enhances intravasation and thereby metastasis formation in the Rag2$^{-/-}$ γc$^{-/-}$ mice.

Finally, we determined whether in the Rag2$^{-/-}$ γc$^{-/-}$ mouse model ErbB1 mediated enhanced lung metastasis was related to increase homing, extravasation, or growth of the tumor cells in the lungs. For this purpose we compared the

MTLn3-GFP and MTLn3-GFP-ErbB1 lung metastasis properties in an experimental metastasis model. Thus, cells were injected into the lateral tail vein (200,000 cells) of 5- to 7-week-old female Rag mice. Four weeks later, the mice were sacrificed, and the lungs were removed and examined for metastases. While in the spontaneous metastasis assay significantly more metastases were observed in the MTLn3-GFP-ErbB1 transplanted group (Fig. 1 and 2), animals receiving MTLn3-GFP or MTLn3-GFP-ErbB1 cells in the tail vein formed a comparable number of metastatic lesions in the lungs (Fig. 3C and D). These results indicate that the enhanced ErbB1 dependent metastasis formation from the primary tumor is rather related to intravasation and/or enhanced invasion than homing events at the target organ.

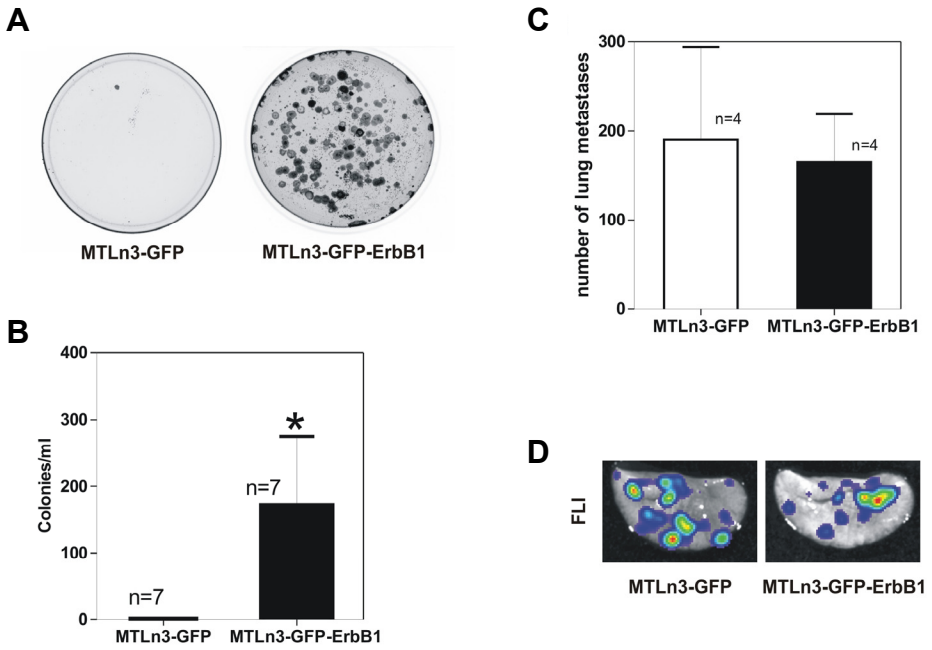

Figure 3: ErbB1-driven metastasis is due to enhanced intravasation ability and not due to enhanced growth of metastases in the lungs. (A) Scan with Typhoon imager of two dishes where approximately 0.7 mL of blood directly drawn from the right ventricule was cultured for 7 days. GFP colonies of blood collected from MTLn3-GFP inoculated mouse (left side) and from MTLn3-GFP-ErbB1 inoculated mouse (right side). (B) Tumor blood burden at the end point of the spontaneous metastasis assay. Colonies were counted after 7 days of culture (MTLn3-GFP versus MTLn3-GFP-ErbB1, $P<0.05$). (C) Lung metastases counted with a fluorescent microscope at x10 magnification (only one side of the left lung) at the end point (day 28) of the experimental metastasis assays (tail vein MTLn3-GFP versus tail vein MTLn3-GFP-ErbB1, $P>0.05$). (D) Lung metastases visualized with the FLI after experimental metastasis assay with the MTLn3-GFP and MTLn3-GFP-ErbB1 cells only.

Strain	Adaptive immunity	Innate immunity	Ref
BALB/c nu/nu 6 **[Nude]**	T cell deficiency		48
CB17/lcr-Prkdc^{scid}/Crl **[Scid]**	T and B cell deficiency		49-51
CB17/lcr.Cg-Prkdc^{scid} Lyst^{bg}/Crl **[Scid Beige]**	T and B cell deficiency	Reduced NK cell function	33,34,52
Rag2$^{-/-}$ γc$^{-/-}$ **[Rag]**	T and B cell deficiency	NK cell deficiency	6,32,53,54

Table 1: Characteristics of immunodeficient mice used

3.3 NK cells do not interfere with primary tumor growth

Previously, we demonstrated the negative role of NK immune cells in lung metastasis formation in Fischer 344 rats[27]. We analyzed several immune deficient mouse models for their capacity to support orthotopic breast cancer metastasis formation. Since ErbB1 enhances intravasation of MTLn3 tumor cells and GFP enables Fluorescent Imaging (FLI) and easy counting of individual lung metastases[14,30,31],we used the MTLn3-GFP-ErbB1 cell line to screen for the most suitable orthotopic breast/tumor metastasis model. We selected 4 mouse strains with different immunodeficiency backgrounds (see Table 1). The conventional nude mice still possess B lymphocytes and NK cells. Severe combined immunodeficiency (SCID) mice lack T and B cells but have NK cells. SCID Beige mice also lack NK cells[6,18,20,21,23,25,32]. Rag2$^{-/-}$ γc$^{-/-}$ mice lack both the adaptive and innate immune response. The common gamma (γc) knock-out mouse lacks functional receptors for many cytokines including IL-2, IL-4, IL-7, IL-9 and IL-15. As a consequence, lymphocyte development is greatly compromised and NK cells are not present. Elimination of the residual T and B cells in the γc$^{-/-}$ background is obtained by crossing these mice to the recombinase activating gene 2 (Rag2) deficient mice[6,32]. All the mice were injected with 500,000 MTLn3-GFP-ErbB1 cells in the right thoracic mammary fat pad. We followed the primary tumor growth for 4 weeks and sacrificed the mice when the tumors reached an average size of 10 mm by 10 mm. The primary tumor growth in all mice strains except for the Scid Beige did have similar rate. The xenografts in the Scid Beige seem to show a delayed growth but the difference with the other mouse strains is not significant and most of all the average tumor weight was comparable with the other three mouse strains (Fig. 4A and B). Overall the primary tumor volume varied between 300 and 500 mm^3 (Fig. 4A) and tumor weight between 300 and 500 mg (Fig. 4B). Both volume and weight were not significantly different between the 4 mouse strains. No difference was noticed in tumor organization, as determined by H&E staining (data not shown). No necrotic region was observed in all the tumors of the different mice strains. Since there is no significant difference in tumor weight

especially between the Scid and the Scid Beige, the results suggest that NK cells do not interfere with the tumor growth of the MTLn3-GFP-ErbB1 cells.

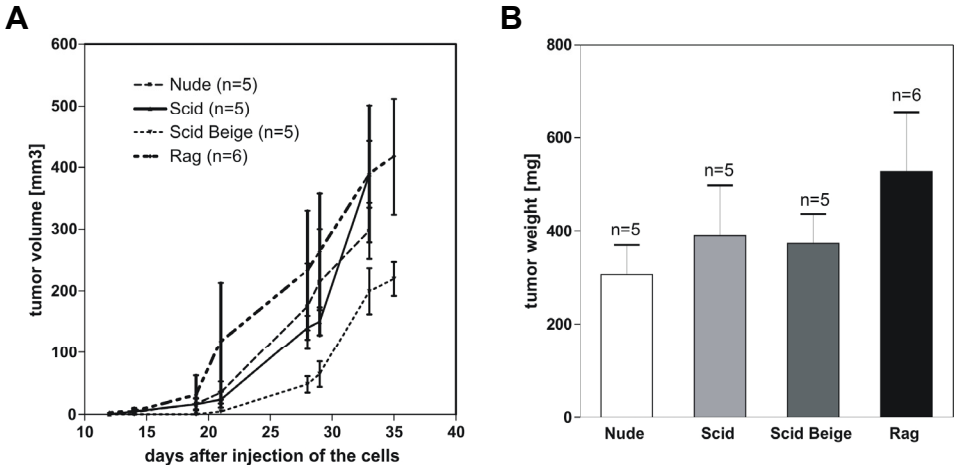

Figure 4: MTLn3-GFP-ErbB1 cells have similar growth rate in Nude, Scid, Scid Beige and Rag2$^{-/-}$ γc$^{-/-}$ mice (A) Tumor growth rate monitored in the Nude (n=5), Scid (n=5), Scid Beige (n=5) and Rag2 $^{-/-}$ γc $^{-/-}$ (n=6) mice by measuring the volume over the time period of the experiment. (B) Primary tumor weight at the end point of the spontaneous metastasis assay (P>0.05).

3.4 Efficient orthotopic lung metastasis formation in the Rag2 $^{-/-}$ γc $^{-/-}$ and Scid Beige mice

After orthotopic transplantation of MTLn3 cells into the mammary gland of the 4 different mouse strains, a primary tumor formed in every mouse. Next we checked for the number of lung metastases after sacrificing the mice. The presence of GFP in the MTLn3 cells allowed the quantification of the lung metastases and classification according to their size by fluorescence microscopy (Fig. 5B). While there was no significant difference in primary tumor growth in all the 4 different mouse strains (Fig. 4), almost no lung metastases were observed in either nude or SCID mice (Fig. 5A). Many lung metastases were observed in both Rag2$^{-/-}$ γc$^{-/-}$ and Scid Beige mice, although the latter showed significantly fewer metastases than the Rag2$^{-/-}$ γc$^{-/-}$ mice (Fig. 5A). Visualization of individual metastases by immunofluorescence microscopy demonstrated that in the Scid Beige mice the size of the metastases ranged from less than 0,1 mm^2 to 0,3 mm^2 while in the Rag2$^{-/-}$ γc$^{-/-}$ mice they were all above 0,3 mm^2 (Fig. 5B). When the lungs are injected with ink, it was not possible to observe metastases in the Scid Beige; they are only visible with HE staining. However metastases were clearly visible in the Rag2$^{-/-}$ γc$^{-/-}$ mice (Fig. 5C). Since NK cells are still present in both nude and Scid mice but are absent in both Scid Beige and Rag2$^{-/-}$ γc$^{-/-}$ mice, it shows that the presence of NK cells is the limiting factor for efficient lung metastasis formation in orthotopic breast

cancer models. Furthermore, the beige mutation not only results in loss of cytotoxic T cells and selective impairment of NK cell functions but also in macrophage defects which could explain the lower average tumor weight and most probably the reduced number of lung metastases in the Scid Beige mice compared with the Rag2$^{-/-}$ γc$^{-/-}$ mice[33,34], since macrophages are important for MTLn3 lung metastasis formation.

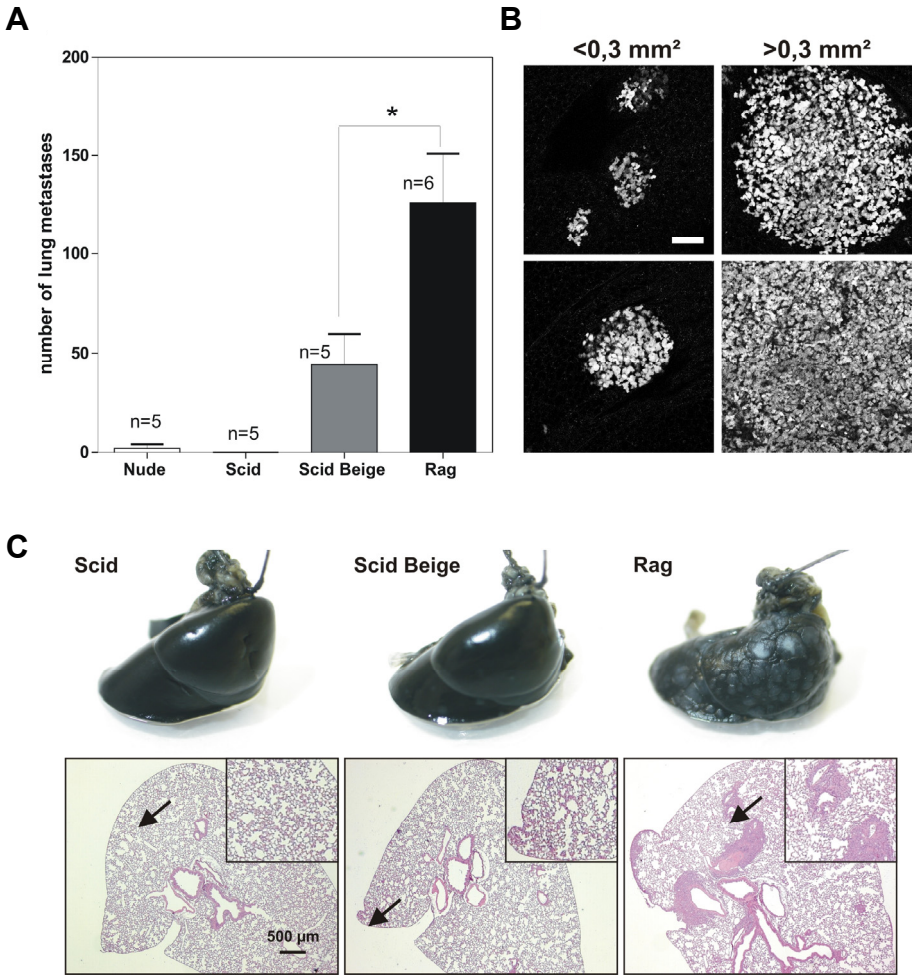

Figure 5: NK cells interfere with lung metastasis formation. After sacrifice, the number of GFP-positive lung metastases was counted ex vivo using an inverted fluorescent microscope and a x10 objective lens. (A) Number of lung metastases at the end point of the spontaneous metastasis assay (t-test, $p<0.05$). (B) Images of the four different sizes of lung metastases encountered during counting. Bar represents 100 µm. (C) After 5 weeks, lungs were isolated, injected with ink (right lobes) and lung (left lobe) sections were stained with H&E.

3.5 Efficient orthotopic lung metastasis formation in the Rag2 $^{-/-}$ γc $^{-/-}$ using the 4T1-luc cell-line

Orthotopic transplantation of MTLn3-GFP-ErbB1 cells into the mammary gland of Rag2$^{-/-}$ γc$^{-/-}$ mice resulted in a high number of lung metastases. Next we checked whether indeed the Rag2$^{-/-}$ γc$^{-/-}$ mouse is also a good recipient for another highly metastatic cell-line, the 4T1-luc cell-line. This cell-line is supposed to metastasize easily to the lungs and other target organs in the syngeneic orthotopic mouse model the Balb/c mouse[35]. We injected 100,000 4T1-luc cells in the T4 mammary fat pad of both Rag2$^{-/-}$ γc$^{-/-}$ and Balb/c mice. In the time scale of 3 weeks, the tumor growth was significantly faster in the Rag2$^{-/-}$ γc$^{-/-}$ mice (Fig. 6A) due to the immune system of the Balb/c mouse. At time of sacrifice, the tumor weight was similar in both mouse strains (Fig. 6B), however there were significantly many more and large lung metastases in the Rag2$^{-/-}$ γc$^{-/-}$ mice than in the Balb/c mice (Fig. 6C and D). In three weeks time, we could only observe a high number of lung metastases formed by 4T1-luc cells in the Rag2$^{-/-}$ γc$^{-/-}$ mouse model which makes it a suitable breast cancer mouse model.

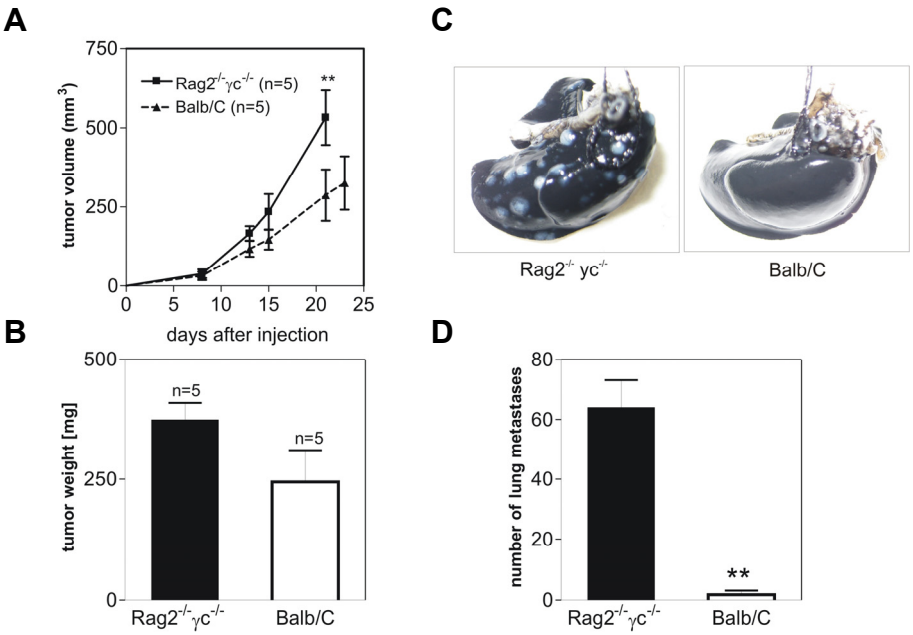

Figure 6: 4T1-luc cells metastasize more efficiently in the Rag2$^{-/-}$ γc$^{-/-}$ mice than in their syngeneic mouse model the Balb/c. (A) Tumor growth rate of the 4T1 cells monitored in the Rag2 $^{-/-}$ γc $^{-/-}$ mice (n=5) and in the Balb/C mice (n=5) during three weeks. (B) Primary tumor weight at the end point of the spontaneous metastasis assay (P>0.05). (C) Example of lung injected with ink (right lobe) to show number and size of metastases in both mouse models. (D) Lung metastases at the end point of the spontaneous metastasis assay (t-test, p=0.0040).

4. **Discussion**

Modeling metastasis *in vivo* is a true challenge but necessary for studying mechanisms underlying the tumor cell biological processes (e.g. cell migration) that enable certain cells to spread to other parts of the body [7]. EGFR-signaling is a pathway that is known to be involved in breast tumor progression. We checked whether EGFR overexpression in MTLn3 cells results in increased number of lung metastases in the Rag2$^{-/-}$ γc$^{-/-}$ mice. Our data indicate that increased expression of ErbB1 in the MTLn3 mammary adenocarcinoma cells results in slower primary tumor growth which is in contradiction with previous findings[12,13,16]. Since *in vitro,* MTLn3-GFP-ErbB1 cells show an increased proliferation activity compared with control cells, a logical and easy explanation could be a difference in cell survival. Indeed, when cultured at high density MTLn3-GFP-ErbB1 cells suffer and eventually die due to contact inhibition, while MTLn3-GFP control cells survive more easily cell-cell contact. MTLn3-GFP-ErbB1 cells may suffer more from the fat pad injection procedure which means that fewer cells survive and only a reduced number of cells is able to grow out in a primary tumor.

ErbB1 overexpression enhances the ability to intravasate and, thus, provides sufficient seeding capacity to allow lung metastases formation in the Rag2$^{-/-}$ γc$^{-/-}$ mice. Indeed, there were an increased number of tumor cells in the circulation of mice with ErbB1-expressing tumors, while few cells could be detected in the blood collected from control tumor bearing mice. Furthermore, the efficiency of the lung colonization by MTLn3 cells (experimental metastasis assay) was similar whether ErbB1 was over expressed or not. These results are consistent with previous *in vivo* studies showing that ErbB1 expression can enhance invasiveness most probably through increased chemotaxis to gradients of EGF[36,37]. The CD31 staining which is a marker for angiogenesis did not reveal difference in blood vessels density through the primary tumor of both groups (data not shown). The presence of macrophages in the Rag2$^{-/-}$ γc$^{-/-}$ mice allows the paracrine loop with tumor cells to take place and thus enhances invasiveness in response to EGF.

In this study, we have shown that the presence of remaining innate immune cells including NK cells in the nude and severe compromised immunodeficient (SCID) mouse does not affect the growth of the primary tumor but inhibits the formation of lung metastases[6,17,27,38]. Indeed, we have found that the Rag2 $^{-/-}$ γc$^{-/-}$ mouse which lacks NK cells is an excellent recipient animal model to study breast tumor formation and progression when using the MTLn3 overexpressing ErbB1 cells or the 4T1 cells. Previous reports demonstrated the contribution of NK cells in tumor growth and metastasis[27,39-42]. In particular Dewan MZ and colleagues demonstrated the direct role of NK cells in tumor growth and metastasis using NOD/SCID/γc^{null} (NOG) mice lacking T, B and NK cells which are similar with the Rag2$^{-/-}$ γc$^{-/-}$ mice used in our study[43]. They showed both increased efficiency of engraftment and spontaneous metastasis of the human breast cancer cell-line MB-MDA-231 in the NOG mice pointing out that the NK

cells play a critical role in tumor growth and metastasis [44]. In our study, we used the rat mammary adenocarcinoma MTLn3 cell-line overexpressing ErbB1 and did not find that the NK cells play a significant role in engraftment and primary tumor growth but only in the formation of spontaneous lung metastases. Since the Rag2$^{-/-}$ γc$^{-/-}$ and NOG mice have similar immunodeficiencies, i.e. T, B, and NK cell reductions, one might expect similar results for the NOG mouse as for the Rag2$^{-/-}$ γc$^{-/-}$ mouse. Zhang and colleagues also conclude that Rag2$^{-/-}$ γc$^{-/-}$ mice similar to NOD/SCID/γc^{null} (NOG) mice provide excellent immunodefficient setting for human engraftment[45]. Nevertheless, our results concerning efficient engraftment of the tumor cells do not show that NK cells play a role in this tumor progression step. Tumor growth in the SCID Beige mice was a bit delayed but they lack NK cells as well. In fact, the beige mutation not only results in loss of cytotoxic T cells and selective impairment of NK cell functions but also in macrophage defects which could explain the lower average tumor weight and most probably the reduced number of lung metastases[33,34]. Indeed, it has been shown that macrophages can form a paracrine loop with tumor cells to enhance invasiveness in response to EGF stimulation[36,37,46,47]. So the defective macrophages in SCID Beige mice could be the reason why tumor growth and number of lung metastases was reduced in comparison with the Rag mice. In addition, we also tested the 4T1 mouse mammary tumor cell-line, one of the only few breast cancer models with the capacity to metastasize efficiently to sites affected in human breast cancer. When introduced orthotopically in the syngeneic Balb/c mouse model with complete immune system, 4T1 are capable of metastasis to several organs affected in breast cancer[12,13,35]. However, when we injected the 4T1-luc cells in the Rag2$^{-/-}$ γc$^{-/-}$ and Balb/c mice, we could only detect lung metastases in the Rag2$^{-/-}$ γc$^{-/-}$ mice although a primary tumor formed in both mouse strains. Even after three weeks of experiment the primary tumor started to shrink in the Balb/c mice. In conclusion, our results suggest that NK cells play an important role in inhibiting metastasis formation but not in tumor growth. Since metastasis formation in breast cancer patients is the most significant problem, enhancing NK activity could be a promising immunotherapeutic strategy against the spread of cancer to target organs. Moreover to validate the target genes found to have a crucial role in cell migration and intravasation in the Rag/MTLn3 model, a complementary model could be the use of the 4T1 syngeneic metastatic breast cancer model.

In summary, ErbB1 overexpression in the MTln3 cells did delay the primary tumor growth but was essential for efficient intravasation and lung metastasis formation. This suggests a preferential role of ErbB1 expression in tumor cells to (in)directly drive the biological processes that are essential in the intravasation process, such as cell motility. Second, we demonstrated that the Rag mouse model which lacks T, B and NK cells but not the macrophages is a clinically relevant animal model when using MTLn3 and 4T1 tumor cells to understand and investigate the mechanism of breast cancer cell growth and metastasis. We provide

evidence for the crucial role of the NK cells in metastasis formation but not in tumor growth. In conclusion, we established an improved breast cancer animal model by using the Rag2$^{-/-}$ $\gamma c^{-/-}$ mouse strain together with MTLn3 cells overexpressing human ErbB1 receptors. This improved model system described in the present study may provide a novel opportunity to understand and investigate the mechanism of tumor growth and metastasis.

Acknowledgments

We thank Jeffrey E. Segall for the GFP-MTLn3-ErbB1 cells, valuable discussion and critically reading of the manuscript. This work was financially supported by grants from the Dutch Cancer Society (UL 2006-3538 and UL 2007-3860), the EU FP7 Health Program Metafight (Grant agreement no.201862), the Netherlands Organization for Scientific Research (902-21-229 and 911-02-022) and TI Pharma (T3-107).

SUPPLMENTAL DATA

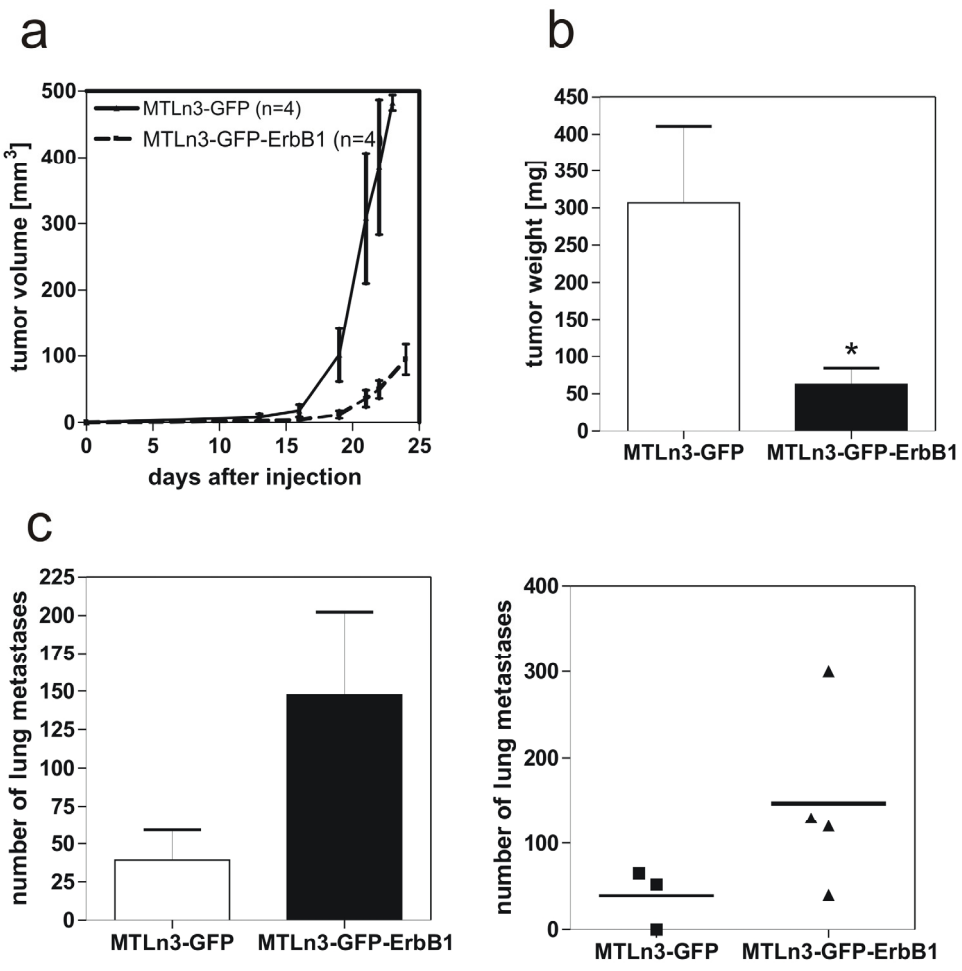

Figure S1: ErbB1 over-expression delays tumor growth but enhances lung metastasis formation in the Rag2$^{-/-}$ γc$^{-/-}$ mice. (A) Primary tumor growth measured by caliper during spontaneous metastasis assay. Rag mice were inoculated with MTLn3-GFP (n=4) and MTLn3-GFP-ErbB1 (n=4). (B) Primary tumor weight at the end point of the spontaneous metastasis assay. The mice were sacrificed exactly 25 days after fat pad injection. ($p<0.05$). (C) Number of lung metastases counted with a fluorescent microscope at x10 magnification at the end point (day 25) of the spontaneous metastasis assays ($p>0.05$).

REFERENCE LIST

1. Ferlay, J.; Autier, P.; Boniol, M. et al. Estimates of the cancer incidence and mortality in Europe in 2006. Ann.Oncol. 18: 581-592, 2007.
2. Pantel, K.; Brakenhoff, R. H. Dissecting the metastatic cascade. Nat.Rev.Cancer. 4: 448-456, 2004.
3. Gupta, G. P.; Massague, J. Cancer metastasis: building a framework. Cell. 127: 679-695, 2006.
4. van Nimwegen, M. J.; van de, W. B. Focal adhesion kinase: a potential target in cancer therapy. Biochem.Pharmacol. 73: 597-609, 2007.
5. Vargo-Gogola, T.; Rosen, J. M. Modelling breast cancer: one size does not fit all. Nat.Rev.Cancer. 7: 659-672, 2007.
6. Cao, X.; Shores, E. W.; Hu-Li, J. et al. Defective lymphoid development in mice lacking expression of the common cytokine receptor gamma chain. Immunity. 2: 223-238, 1995.
7. Khanna, C.; Hunter, K. Modeling metastasis in vivo. Carcinogenesis. 26: 513-523, 2005.
8. Sharpless, N. E.; Depinho, R. A. The mighty mouse: genetically engineered mouse models in cancer drug development. Nat.Rev.Drug Discov. 5: 741-754, 2006.
9. Ottewell, P. D.; Coleman, R. E.; Holen, I. From genetic abnormality to metastases: murine models of breast cancer and their use in the development of anticancer therapies. Breast Cancer Res.Treat. 96: 101-113, 2006.
10. Neri, A.; Welch, D.; Kawaguchi, T.; Nicolson, G. L. Development and biologic properties of malignant cell sublines and clones of a spontaneously metastasizing rat mammary adenocarcinoma. J.Natl.Cancer Inst. 68: 507-517, 1982.
11. Marxfeld, H.; Staedtler, F.; Harleman, J. H. Characterisation of two rat mammary tumour models for breast cancer research by gene expression profiling. Exp.Toxicol.Pathol. 58: 133-143, 2006.
12. Hynes, N. E.; Lane, H. A. ERBB receptors and cancer: the complexity of targeted inhibitors. Nat.Rev.Cancer. 5: 341-354, 2005.
13. Giancotti, V. Breast cancer markers. Cancer Lett. 243: 145-159, 2006.
14. Condeelis, J.; Segall, J. E. Intravital imaging of cell movement in tumours. Nat.Rev.Cancer. 3: 921-930, 2003.
15. Condeelis, J.; Singer, R. H.; Segall, J. E. The great escape: when cancer cells hijack the genes for chemotaxis and motility. Annu.Rev.Cell Dev.Biol. 21: 695-718, 2005.
16. Xue, C.; Wyckoff, J.; Liang, F. et al. Epidermal growth factor receptor overexpression results in increased tumor cell motility in vivo coordinately with enhanced intravasation and metastasis. Cancer Res. 66: 192-197, 2006.
17. Cerwenka, A.; Lanier, L. L. Natural killer cells, viruses and cancer. Nat.Rev.Immunol. 1: 41-49, 2001.
18. Garofalo, A.; Chirivi, R. G.; Scanziani, E. et al. Comparative study on the metastatic behavior of human tumors in nude, beige/nude/xid and severe combined immunodeficient mice. Invasion Metastasis. 13: 82-91, 1993.
19. Sharkey, F. E.; Fogh, J. Incidence and pathological features of spontaneous tumors in athymic nude mice. Cancer Res. 39: 833-839, 1979.
20. Sebesteny, A.; Taylor-Papadimitriou, J.; Ceriani, R. et al. Primary human breast carcinomas transplantable in the nude mouse. J.Natl.Cancer Inst. 63: 1331-1337, 1979.
21. Rae-Venter, B.; Reid, L. M. Growth of human breast carcinomas in nude mice and subsequent establishment in tissue culture. Cancer Res. 40: 95-100, 1980.
22. Phillips, R. A.; Jewett, M. A.; Gallie, B. L. Growth of human tumors in immune-deficient scid mice and nude mice. Curr.Top.Microbiol.Immunol. 152: 259-263, 1989.
23. Zietman, A. L.; Sugiyama, E.; Ramsay, J. R. et al. A comparative study on the xenotransplantability of human solid tumors into mice with different genetic immune deficiencies. Int.J.Cancer. 47: 755-759, 1991.
24. Kubota, T.; Yamaguchi, H.; Watanabe, M. et al. Growth of human tumor xenografts in nude mice and mice with severe combined immunodeficiency (SCID). Surg.Today. 23: 375-377, 1993.

25. Clarke, R. Human breast cancer cell line xenografts as models of breast cancer. The immunobiologies of recipient mice and the characteristics of several tumorigenic cell lines. Breast Cancer Res.Treat. 39: 69-86, 1996.
26. van Nimwegen, M. J.; Verkoeijen, S.; van Buren, L.; Burg, D.; van de, W. B. Requirement for focal adhesion kinase in the early phase of mammary adenocarcinoma lung metastasis formation. Cancer Res. 65: 4698-4706, 2005.
27. van Nimwegen, M. J.; Verkoeijen, S.; Kuppen, P. J.; Velthuis, J. H.; van de, W. B. An improved method to study NK-independent mechanisms of MTLn3 breast cancer lung metastasis. Clin.Exp.Metastasis. 2007.
28. Neri, A.; Nicolson, G. L. Phenotypic drift of metastatic and cell-surface properties of mammary adenocarcinoma cell clones during growth in vitro. Int.J.Cancer. 28: 731-738, 1981.
29. Huigsloot, M.; Tijdens, I. B.; Mulder, G. J.; van de, W. B. Differential regulation of doxorubicin-induced mitochondrial dysfunction and apoptosis by Bcl-2 in mammary adenocarcinoma (MTLn3) cells. J.Biol.Chem. 277: 35869-35879, 2002.
30. Condeelis, J. S.; Wyckoff, J.; Segall, J. E. Imaging of cancer invasion and metastasis using green fluorescent protein. Eur.J.Cancer. 36: 1671-1680, 2000.
31. Wyckoff, J. B.; Jones, J. G.; Condeelis, J. S.; Segall, J. E. A critical step in metastasis: in vivo analysis of intravasation at the primary tumor. Cancer Res. 60: 2504-2511, 2000.
32. Shinkai, Y.; Rathbun, G.; Lam, K. P. et al. RAG-2-deficient mice lack mature lymphocytes owing to inability to initiate V(D)J rearrangement. Cell. 68: 855-867, 1992.
33. Roder, J.; Duwe, A. The beige mutation in the mouse selectively impairs natural killer cell function. Nature. 278: 451-453, 1979.
34. Roder, J. C. The beige mutation in the mouse. I. A stem cell predetermined impairment in natural killer cell function. J.Immunol. 123: 2168-2173, 1979.
35. Tao, K.; Fang, M.; Alroy, J.; Sahagian, G. G. Imagable 4T1 model for the study of late stage breast cancer. BMC.Cancer. 8: 228-2008.
36. Wyckoff, J.; Wang, W.; Lin, E. Y. et al. A paracrine loop between tumor cells and macrophages is required for tumor cell migration in mammary tumors. Cancer Res. 64: 7022-7029, 2004.
37. Wyckoff, J. B.; Wang, Y.; Lin, E. Y. et al. Direct visualization of macrophage-assisted tumor cell intravasation in mammary tumors. Cancer Res. 67: 2649-2656, 2007.
38. Wu, J.; Lanier, L. L. Natural killer cells and cancer. Adv.Cancer Res. 90: 127-156, 2003.
39. Ben Eliyahu, S.; Page, G. G.; Yirmiya, R.; Taylor, A. N. Acute alcohol intoxication suppresses natural killer cell activity and promotes tumor metastasis. Nat.Med. 2: 457-460, 1996.
40. Ben Eliyahu, S.; Page, G. G.; Yirmiya, R.; Shakhar, G. Evidence that stress and surgical interventions promote tumor development by suppressing natural killer cell activity. Int.J.Cancer. 80: 880-888, 1999.
41. Bouzahzah, B.; Albanese, C.; Ahmed, F. et al. Rho family GTPases regulate mammary epithelium cell growth and metastasis through distinguishable pathways. Mol.Med. 7: 816-830, 2001.
42. Melamed, R.; Rosenne, E.; Shakhar, K. et al. Marginating pulmonary-NK activity and resistance to experimental tumor metastasis: suppression by surgery and the prophylactic use of a beta-adrenergic antagonist and a prostaglandin synthesis inhibitor. Brain Behav.Immun. 19: 114-126, 2005.
43. Dewan, M. Z.; Terunuma, H.; Ahmed, S. et al. Natural killer cells in breast cancer cell growth and metastasis in SCID mice. Biomed.Pharmacother. 59 Suppl 2: S375-S379, 2005.
44. Beckhove, P.; Schutz, F.; Diel, I. J. et al. Efficient engraftment of human primary breast cancer transplants in nonconditioned NOD/Scid mice. Int.J.Cancer. 105: 444-453, 2003.
45. Zhang, B.; Duan, Z.; Zhao, Y. Mouse models with human immunity and their application in biomedical research. J.Cell Mol.Med. 2008.
46. Condeelis, J.; Pollard, J. W. Macrophages: obligate partners for tumor cell migration, invasion, and metastasis. Cell. 124: 263-266, 2006.
47. Robinson-Smith, T. M.; Isaacsohn, I.; Mercer, C. A. et al. Macrophages mediate inflammation-enhanced metastasis of ovarian tumors in mice. Cancer Res. 67: 5708-5716, 2007.

48. Gershwin, M. E.; Merchant, B.; Gelfand, M. C. et al. The natural history and immunopathology of outbred athymic (nude) mice. Clin.Immunol.Immunopathol. 4: 324-340, 1975.
49. McCune, J. M.; Namikawa, R.; Kaneshima, H. et al. The SCID-hu mouse: murine model for the analysis of human hematolymphoid differentiation and function. Science. 241: 1632-1639, 1988.
50. Dorshkind, K.; Pollack, S. B.; Bosma, M. J.; Phillips, R. A. Natural killer (NK) cells are present in mice with severe combined immunodeficiency (scid). J.Immunol. 134: 3798-3801, 1985.
51. Schuler, W.; Bosma, M. J. Nature of the scid defect: a defective VDJ recombinase system. Curr.Top.Microbiol.Immunol. 152: 55-62, 1989.
52. Mosier, D. E.; Stell, K. L.; Gulizia, R. J.; Torbett, B. E.; Gilmore, G. L. Homozygous scid/scid;beige/beige mice have low levels of spontaneous or neonatal T cell-induced B cell generation. J.Exp.Med. 177: 191-194, 1993.
53. Colucci, F.; Soudais, C.; Rosmaraki, E. et al. Dissecting NK cell development using a novel alymphoid mouse model: investigating the role of the c-abl proto-oncogene in murine NK cell differentiation. J.Immunol. 162: 2761-2765, 1999.
54. Greenberg, P. D.; Riddell, S. R. Deficient cellular immunity--finding and fixing the defects. Science. 285: 546-551, 1999.